

Fabrication of Omniphobic-Omniphilic Micropatterns using GPOSS-PDMS Coating

Dmitrii D. Kartsev, Artur Y. Prilepskii, Iliia M. Lukyanov, Eduard G. Sharapenkov, Anastasiia V. Klaving, Aleksandr Goltaev, Alexey Mozharov, Liliia Dvoretckaia, Ivan Mukhin, and Pavel A. Levkin*

Surfaces with special wettability properties, such as omniphobicity or omniphilicity, are essential for functional devices that use both aqueous and organic media. Micropatterning of omniphobic and omniphilic properties can provide a wide range of applications, including miniaturized experiments using both aqueous and organic media. Herein, an approach for creating omniphobic-omniphilic micropatterns based on selective photoacid polymerization of octa(3-glycidylpropyl) polyhedral oligomeric silsesquioxane modified with mono-aminopropyl-terminated polydimethylsiloxane is reported. The composition of the polymeric coatings using infrared spectroscopy; patterning accuracy using atomic force microscopy and scanning electron microscopy; wettability characteristics of the omniphobic, and omniphilic surfaces using contact angle measurements are studied. The proposed approach allows for single-step micropatterning (sub-10 μm) or macropatterning (3 mm). Liquids with surface tensions $>22.8 \text{ mN m}^{-1}$ can be confined to the omniphilic areas by the omniphobic borders. C2C12 cells are successfully cultivated in omniphilic areas, demonstrating their cell compatibility. The cells adhere to and grow on the entire surface of the pattern, without any signs of cytotoxicity. However, the strongest adhesion is observed in the omniphilic areas, making it possible to create cell micropatterns in a single step. The proposed method for the fabrication of omniphobic-omniphilic transparent, mechanically robust, biocompatible patterns can find applications in microfluidics, biotechnology or miniaturized biological screening experiments.

1. Introduction

Omniphobic surfaces are repellent to both water and low surface tension liquids,^[1,2] demonstrating low contact angle hysteresis and low sliding angles for water and liquids with lower surface tension.^[2,3] Liquid-repellent surfaces have been within the scope of modern material science for several decades. Special wettability properties allow their application as anti-icing,^[4] self-cleaning,^[5] and anti-biofouling surfaces.^[6] To date, several methods have been developed to construct omniphobic surfaces.^[7–10] These include slippery liquid-infused porous surfaces (SLIPS),^[8] slippery omniphobic covalently attached liquid (SOCAL),^[9] and NanoPools of a Grafted Lubricating Liquid Ingredient for Dewetting Enablement (NP-GLIDE).^[10]

The fabrication of surface micropatterns that combine areas of opposite wettability has multiple applications. Droplet microarrays (DMA) formed using different types of wettability patterns are a powerful method for miniaturizing various types of high-throughput chemical and biological experiments.^[11–14] The hydrophobic,

D. D. Kartsev, A. Y. Prilepskii, I. M. Lukyanov, E. G. Sharapenkov, A. V. Klaving, I. Mukhin
 ITMO University
 International Institute "Solution Chemistry of Advanced Materials and Technologies" (SCAMT)
 9 Lomonosova St., St. Petersburg 191002, Russia
 A. Goltaev, A. Mozharov, L. Dvoretckaia, I. Mukhin
 St. Petersburg Academic University
 Nanotechnology Research and Education Center
 8/3 Khlopin St., St. Petersburg 194021, Russia

 The ORCID identification number(s) for the author(s) of this article can be found under <https://doi.org/10.1002/admi.202300156>.

© 2023 The Authors. Advanced Materials Interfaces published by Wiley-VCH GmbH. This is an open access article under the terms of the Creative Commons Attribution License, which permits use, distribution and reproduction in any medium, provided the original work is properly cited.

DOI: 10.1002/admi.202300156

A. Mozharov
 St. Petersburg State University
 7–9 Universitetskaya Embankment, St. Petersburg 199034, Russia
 I. Mukhin
 Peter the Great St. Petersburg Polytechnic University
 29 Polytechnicheskaya St., St. Petersburg 195251, Russia
 P. A. Levkin
 Karlsruhe Institute of Technology (KIT)
 Institute of Biological and Chemical Systems – Functional Molecular Systems (IBCS-FMS)
 Hermann-von-Helmholtz-Platz 1 76344, Eggenstein-Leopoldshafen, Germany
 E-mail: levkin@kit.edu

superhydrophobic, or omniphobic wettability barriers function as “walls” between liquid droplets and prevent merging and cross-contamination between the droplets. Therefore omniphilic-omniphobic wettability patterns support experiments in media of various surface tensions.^[13,15] Additionally, omniphobic surfaces were shown to possess anti-biofouling properties, which make them perfect barriers in cell-based assays.^[16] However, combining omniphobic and omniphilic properties into precise micropatterns is challenging. Only a few examples of wettability patterning methods that are applicable to both water and low surface tension liquids have been reported. Tuteja and co-workers fabricated a superomniphobic surface by electrospinning solutions of 1H,1H,2H,2H-heptadecafluorodecyl polyhedral oligomeric silsesquioxane and poly(methyl methacrylate) and patterned this surface with omniphilic spots by spatial O₂ plasma treatment.^[17] Lai et al. patterned omniphilic areas on an omniphobic background using site-selective decomposition of 1H,1H,2H,2H-perfluorodecyltriethoxysilane on TiO₂ nanostructured films under UV light.^[18] Feng et al. introduced a two-step synthetic strategy for omniphobic-omniphilic micropatterning utilizing photoinduced thiol-ene reaction.^[19] This method was further improved by combining thiol-ene click modification with the dendrimer approach.^[14] The described methods rely on different strategies for the fabrication of omniphobic barriers. However, to the best of our knowledge, the research on NP-GLIDE for wettability patterning is limited to several works. For example, Zheng et al. demonstrated selective application of NP-GLIDE omniphobic films via UV polymerization.^[20]

The NP-GLIDE approach is based on the incorporation of a liquid-like low surface energy component, typically PDMS^[21] or a perfluorinated ether,^[22] into a polymer matrix. Zhang et al. introduced an NP-GLIDE approach that allows the production of photocurable polymeric coatings with high wear resistance, omniphobic surface properties, and optical transparency.^[10] The photoacid polymerization of the precursor coating containing PDMS-modified octa(3-glycidylpropyl) polyhedral oligomeric silsesquioxane (GPOSS-PDMS) was initiated using triarylsulfonium hexafluoroantimonate salts. A similar approach has been applied in commercial SU-8 photoresists, which are extensively used in various applications.^[23,24] Therefore, we decided to test the hypothesis that GPOSS-PDMS-based composition can be used as an omniphobic photoresist to create wettability patterns.

Herein, we present two new omniphilic-omniphobic patterning methods, both of which are based on the selective photoinduced polymerization of a GPOSS-PDMS colloidal solution on an omniphilic substrate to produce omniphobic GPOSS-PDMS areas. The macropatterning method allowed us to produce wettability patterns with developed features of 1–3 mm in size. The second micropatterning method is meant for high resolution patterning and allows the creation of omniphilic-omniphobic patterns with features as small as 8 μm. We applied this macropatterning method to create DMA of liquids. Omniphilic spots on the omniphobic background could confine droplets of both organic solvents (such as dimethyl sulfoxide (DMSO), dimethylformamide (DMF), and hexadecane), and aqueous solutions. Moreover, we demonstrated the effect of discontinuous dewetting^[19,25] with the formation of droplets upon dragging drops of low-surface-tension liquids or

high-surface-tension aqueous solutions across an array of omniphilic spots. Finally, we demonstrated the selective adhesion of cells to omniphilic areas with facile cell detachment from the omniphobic areas, which was utilized for the formation of live cell patterns.

2. Results and Discussion

2.1. GPOSS-PDMS Film Casting Optimization

The core method of our approach is based on a previously reported NP-GLIDE procedure designed for protective applications, which we adopted and modified to achieve patterning.^[6] First, we reproduced the procedure. GPOSS was modified using linear amino-functionalized PDMS fragments by reacting GPOSS with PDMS-NH₂ in butyl acetate solvent at 120 °C for 1.5 h (Figure 1A(i)). The PDMS-NH₂/GPOSS molar ratio was 1/27 to avoid the attachment of two or more PDMS chains to one GPOSS molecule. The reaction mixture containing both GPOSS monomers and modified monomers was added to acetonitrile, leading to the formation of micelles owing to the amphiphilic nature of GPOSS-PDMS (Figure 1A(ii)). The colloidal solution (Figure 1A(iii)) was used to obtain precursor solutions A and B that were further applied for macro- and micropatterning accordingly (Figure 1B).

We started our optimization process by reducing the coating thickness. Since the initial NP-GLIDE films were intended for protective applications, their thickness was 50–100 micrometers. To reduce the thickness and improve the patterning resolution, we applied GPOSS-PDMS precursor solutions to the substrate surface via spin coating (Figure 1B(i)). To study the relation between the layer thickness and spin-coating parameters we inspected the cross sections of the applied coatings with scanning electron microscopy (SEM) (250 nm for 4000

rpm for 1 min, 300 nm for 3000 rpm for 1 min, 450 nm for 2000 rpm for 1 min, and 750 nm for 1000 rpm for 1 min) (Figure S1, Supporting Information). We selected the parameters corresponding to the formation of the thickest layer (1000 rpm for 1 min) to ensure high mechanical stability of the coating.

Next, we optimized the baking parameters. In the original publication, GPOSS-PDMS-based NP-GLIDE coatings were dried at 75 °C overnight.^[26] In our study, we reduced the baking time because the film layer was thinner. Glass slides spin-coated with the precursor mixture were dried at 80 °C for 10, 20, 30, and 40 min. The static contact angles on slides after 10 min of drying were measured (Table 1) and did not change significantly with increased drying time. Thus, drying for > 10 min was considered ineffective.

The resolution typically decreases with exposure time. Thus, to achieve the highest possible patterning resolution for both methods, we optimized the duration of UV irradiation (Figure 1B(iii)). For macropatterning, dry films of the precursor coating were irradiated with a 125 W mercury vapor lamp (range of wavelengths from 254 to 579 nm, 6.9 mW cm⁻² at a wavelength of 365 nm) from 5 to 9 min (with an increasing step of 1 min) through a chromium glass photomask. No

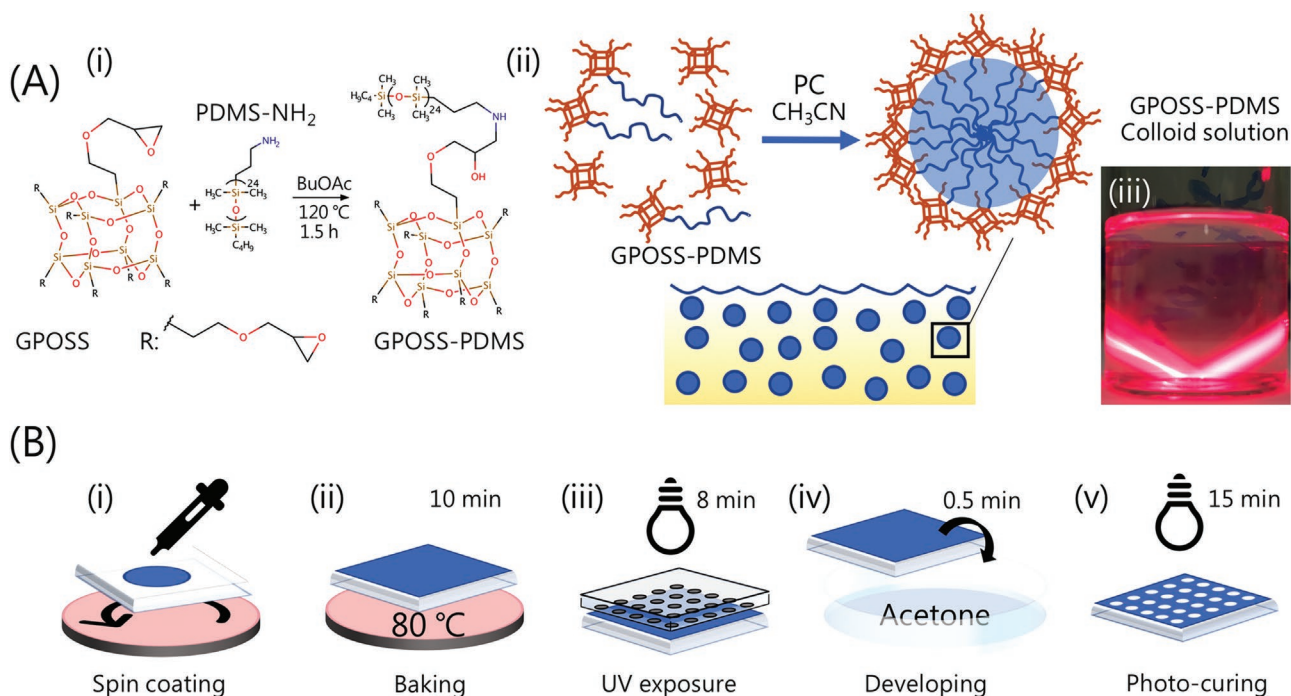


Figure 1. The process of GPOSS-PDMS patterning. A) Preparation of GPOSS-PDMS emulsion. i) Synthesis of GPOSS-PDMS (BuOAc – butyl acetate). ii) Scheme showing the formation of a colloidal solution, in which GPOSS-PDMS acts as a surfactant when added to acetonitrile (PC – propylene carbonate). iii) Photograph showing laser beam scattering, confirming the formation of an emulsion. B) Photolithography process describing GPOSS-PDMS patterning. i) Spin coating at 1000 rpm for 1 min. ii) Baking at 80 °C for 10 min. iii) UV exposure for 8 min. iv) Developing in acetone for 0.5 min. v) Additional photo-curing by UV for 15 min.

significant differences were observed in the FTIR spectra (Figure S2, Supporting Information). All the samples had a residual epoxy group peak at 915 cm^{-1} , which proved polymerization was incomplete. We found that the films exposed to UV light for 5, 6, and 7 min detached from the substrate after flushing with acetone, which was chosen as a developing agent. However, 8 min of irradiation proved to be enough to achieve films stable during acetone rinsing. Following the development step, films were further irradiated with UV for 15 min leading to complete polymerization as evidenced by the disappearance of the band corresponding to the residual epoxy group at 915 cm^{-1} (Figure S3, Supporting Information). Following the described procedure, we created wettability patterns with 1 mm sized omniphilic areas.

To optimize the UV exposure for micropatterning, we exploited the possibility of using a specified photolithography setting including SÜSS MicroTec MJB4 mask-aligner (wave-

length of 365 nm, power of 0.9 mW cm^{-2}) with higher limiting resolution. The UV source in MJB4 is less powerful than the mercury lamp used for the first method, which resulted in the need for additional optimization. Using precursor solution A we did not obtain a stable coating even after 2 h of UV exposure through an aluminum-glass photomask. Therefore, the concentration of the photoinitiator was increased to 25 wt.% with respect to monomers (precursor solution B). The applied coatings of precursor solution B were photolyzed for 15–30 min (in steps of 5 min) through an aluminum-glass photomask. We found that the coatings with an exposure of less than 25 min were partially damaged during development (Figure S4, Supporting Information). Thus, for micropatterns, the coatings of precursor solution B were exposed for 25 min. The photolithography resolution for the chosen parameters was observed to be $7.4 \pm 1.9 \mu\text{m}$ and will be discussed in detail further in Section 3.

Table 1. Static contact angles (θ_{st}) (4 μL droplet volume), contact angle hysteresis (CAH) for water, DMSO, DMF, and ethanol on different surfaces: GPOSS-PDMS, activated glass, and omniphilic surface. Each measurement was repeated five times (mean \pm SD is shown).

Solvent	Surface tension [mN m^{-1}]	θ_{st} GPOSS-PDMS [°]	CAH GPOSS-PDMS [°]	θ_{st} activated glass ^{a)} [°]	θ_{st} omniphilic areas ^{b)} [°]	CAH omniphilic areas [°]
Water	72.7	100.1 \pm 0.2	16 \pm 1	17.3 \pm 0.2	47.1 \pm 0.8	31.2 \pm 0.2
DMSO	43.0	72.4 \pm 0.2	6.9 \pm 0.3	spread	21.0 \pm 0.2	17 \pm 1
DMF	35.3	60.2 \pm 0.3	4.2 \pm 0.2	spread	14.1 \pm 0.5	13 \pm 1
Ethanol (96%)	22.8	34.5 \pm 0.1	2.5 \pm 0.6	spread	spread	–

^{a)}Glass slide surface before coating application; ^{b)}Measured inside a 20 \times 20 mm developed area

2.2. Physico-Chemical Characterization of the Patterns

Thin films of GPOSS-PDMS produced using composition A according to the final optimized method were characterized using IR spectroscopy. ATR-FTIR spectra were acquired after photoacid-initiated polymerization (Figure S3, Supporting Information). The -OH stretching peak at 3426 cm^{-1} and ether C-O-C group band at 1100 cm^{-1} , formed in the process of cationic ring opening of the epoxy groups, were registered, while the epoxy group absorption band at 915 cm^{-1} was absent. In contrast to Zhang's report,^[10] a peak at 1720 cm^{-1} was also observed after total of 23 min UV irradiation. We associate this peak with a carbonyl group, probably formed by C-OH group oxidation.

Contact angle measurements were performed for the omniphobic coatings prepared using composition A, according to the final optimized method (Figure 2). We tested several solvents of various polarity and surface tensions (Table 1). Sliding angles were measured (Figure 2A). Liquids with surface tensions between 22.8 mN m^{-1} (ethanol)^[27] and 43 mN m^{-1} (DMSO) easily slid off the obtained coatings with sliding angles of less than 10° (Figure 2B). The sliding angle for water was between 25° and 60° depending on the droplet volume. As expected, the sliding contact angle increased with surface tension and decreased with droplet volume (Figure 2A). The contact angle hysteresis was estimated to be $<10^\circ$ for the studied organic solvents (Table 1). Static contact angles are presented in Figure 2C.

By design, the proposed wettability pattern represents a selectively applied omniphobic GPOSS-PDMS layer. Glass, which represents the developed areas, is known to be hydrophilic.^[28] However, keeping in mind that glass has relatively high contact

angle hysteresis and sliding angles for several liquids, including water, in this paper we call it omniphilic. To prove the omniphilicity of the developed areas, we measured static contact angles and contact angle hysteresis of various solvents. We used a $20 \times 20\text{ mm}$ square on GPOSS-PDMS omniphobic background pattern for testing. According to the received data, we assume that partial modification of the glass with GPOSS-PDMS precursor composition took place in the photolithography process. This inevitably led to the change in the glass surface wettability characteristics. The static contact angles increased compared to those of the activated glass (see Experimental Section) as it is indicated in Table 1. Nevertheless, a pronounced difference in both static contact angles and contact angle hysteresis exists between GPOSS-PDMS and the developed areas.

In the SEM analysis of the cross-sections of the GPOSS-PDMS films, we also noticed pronounced pores of $12\text{--}48\text{ nm}$ in diameter (Figure S5, Supporting Information). In the previous work of Zhang et al., similar pores were observed (average diameter $10 \pm 1\text{ nm}$) and were attributed to PDMS micelles.^[10] The presence of larger pores may be attributed to the aggregation of micelles caused by the changes in the drying process.^[29]

2.3. Patterning Accuracy

One of our goals was to develop an approach for facile omniphobic-omniphilic patterning. For that we used a custom-built setup based on a 125 W wide spectrum high-pressure mercury vapor lamp. The patterning procedure involved spin-coating of the precursor solution A, followed by drying on a magnetic stirrer at 80°C for 10 min, irradiation of the dry coatings with

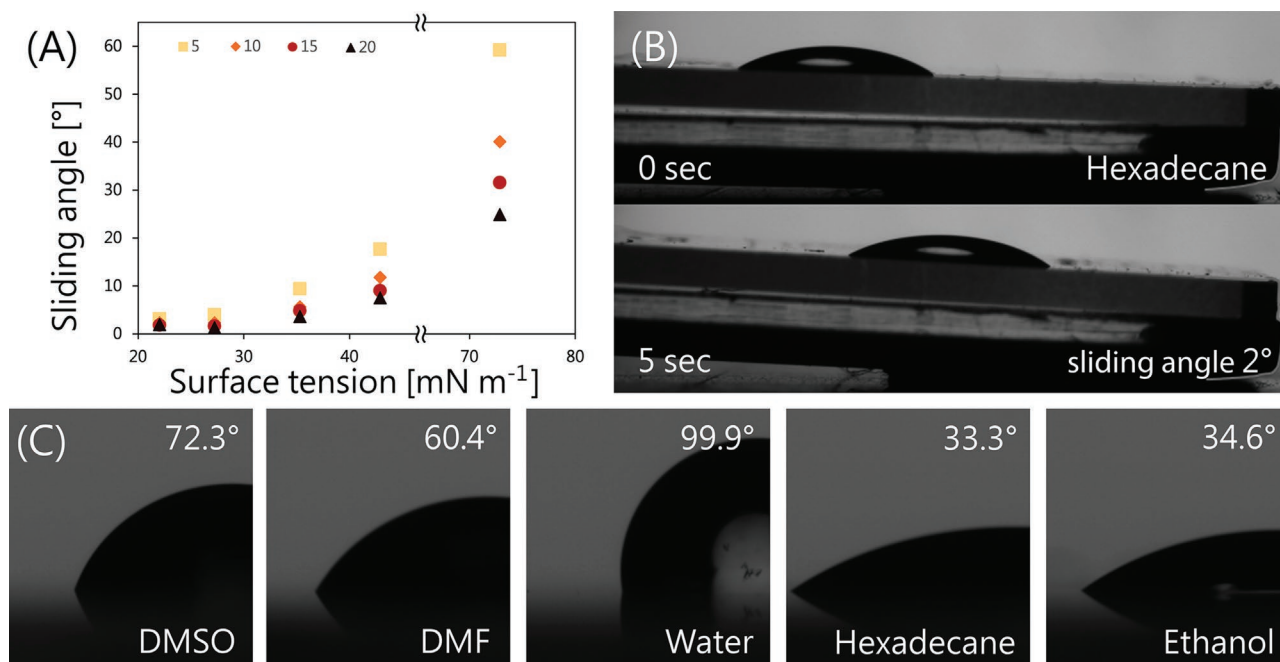


Figure 2. Wettability characteristics of GPOSS-PDMS coatings. A) Dependence of the sliding angle on liquid surface tension for different droplet volumes. B) Measurement of the sliding angle of n-hexadecane (27.5 mN m^{-1}). The sliding angle is $\approx 2^\circ$. No apparent traces of n-hexadecane were observed during sliding. C) Static contact angles of liquids with various surface tensions placed on the omniphobic GPOSS-PDMS coatings. Droplet volume $4\text{ }\mu\text{L}$. Detailed values are listed in Table 1.

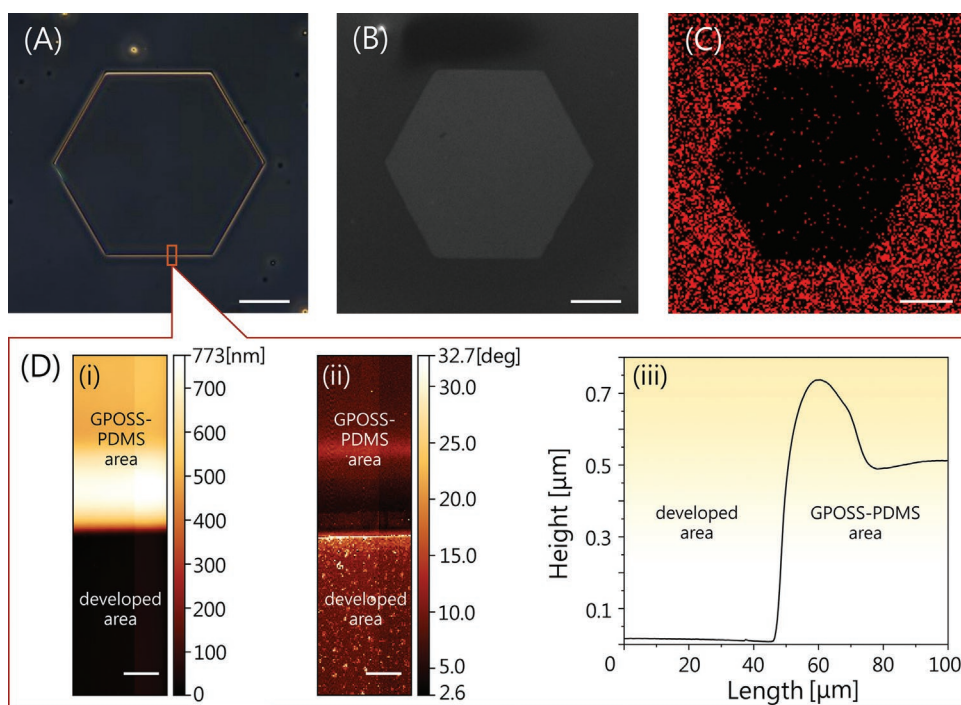


Figure 3. Characterization of microscopic omniphobic-omniphilic patterns. A) Phase-contrast optical image of a hexagonal spot, where the background is UV exposed. Scale bar is 250 μm . B) SEM image of the hexagonal spot. Scale bar is 250 μm . C) Corresponding EDX mapping of the hexagonal spot (carbon K-alpha line signal marked as red). Scale bar is 250 μm . Only $2.1 \pm 1.6\%$ carbon content was observed inside the spot (glass substrate). D) AFM topography image of the hexagonal spot border. A bulge with a height of ≈ 250 nm was found on the border of the spot. Scale bars are 10 μm . i) Border profile. ii) Phase mapping of the spot border. The differences in the phases correspond to different materials inside and outside the spot. iii) AFM topography profile corresponding to the image of the hexagonal spot border (D-i).

UV light through a glass chromium photomask, and development in acetone, followed by an additional 15 min UV. An example of the pattern quality is shown in **Figure 3A**. According to the energy-dispersive X-ray (EDX) mapping (Figure 3B,C), almost the entire GPOSS-PDMS layer was developed inside the omniphilic spots ($2.1 \pm 0.6\%$ carbon content). The average coating thickness was 500 ± 20 nm at a spin-coating speed of 1000 rpm (Figure 3D). The topography of the spot border is shown in Figure 3D(i). According to the atomic force microscopy (AFM) phase images (Figure 3D(ii)), there was a pronounced difference in the phase between the omniphilic spot and the omniphobic coating, confirming the material difference. Notably, the previously measured coating thickness for the spin-coating parameters (Figure S1A, Supporting Information) was ≈ 250 nm greater than that measured after patterning (Figure 3D). We also observed a feature at the border of the spot in the form of a bulge with a height of ≈ 750 nm (Figure 3D(iii)). We assume that the observed result is due to the edge effect occurring at the borders of the photomask, which locally increases the intensity of UV irradiation. This leads to more complete polymerization of the coating at the border of the spot, leading to the formation of bulges. In addition, considering the scale of the length and height (height ≈ 250 nm, length ≈ 30 μm), this bulge does not affect the final patterning parameters.

Method A was not intended for high resolution patterning. With this method we achieved features of 1 mm in size, which is enough to construct wettability patterns for miniaturized test systems.^[12–14] In order to test the resolution of GPOSS-PDMS

photolithography we used a submicron projection photolithography device (MJB4 mask-aligner) for the UV exposure (Figure 4A). In this case precursor solution B was used. As the UV source of the MJB4 was less powerful than the mercury lamp used in method A, the photoinitiator concentration was increased to obtain precursor solution B. Silicon wafers were used as substrates. Atomically smooth Si wafers provide better UV reflection, which improves the accuracy of the exposure process. No organic leftovers from the GPOSS-PDMS composition remained in the omniphilic spots after development, which was confirmed by EDX analysis (Figure 4B,C) ($98.2 \pm 0.6\%$ silicon content). Almost no microdefects were observed in the AFM topography (Figure 4D(i)) and profile images (Figure 4D(iii)) of the omniphilic-omniphobic boundaries. The AFM phase image demonstrates a pronounced difference between the omniphilic and omniphobic areas (Figure 4D(ii)). The smallest lateral dimensions of omniphilic features developed using this method were 74 ± 1.9 μm (Figure S6A, Supporting Information), while the smallest GPOSS-PDMS polymerized features were 5 ± 0.7 μm (Figure S6B, Supporting Information). Thus, we demonstrated that the GPOSS-PDMS photolithography method is suitable for both macro- and micropatterning and allows us to create both omniphobic GPOSS-PDMS structures as small as 8 μm and as thin as 700 nm.

The resolution of photolithography determines the accuracy of the resulting patterns. Thus, the resolution can be further enhanced by using more precise photolithography approaches. We investigated the possibility of using microsphere

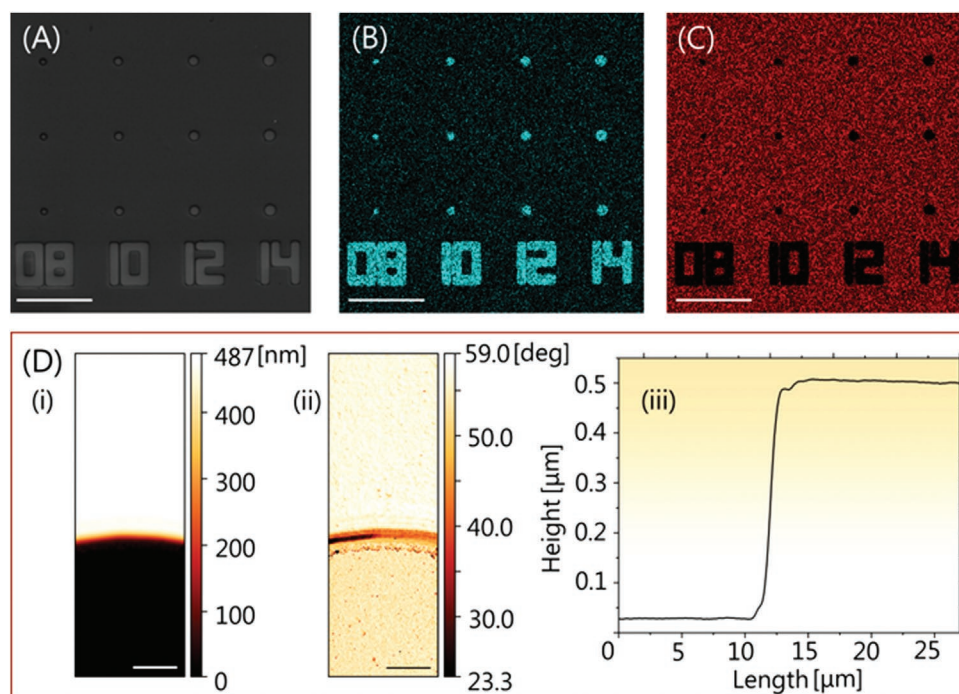


Figure 4. Microscopic study of omniphobic-omniphilic micropatterns. A) SEM image of a micropattern. The numbers represent the circle diameters (μm) in the corresponding rows. Numbers and spots are omniphilic areas with exposed silicon substrate on the GPOSS-PDMS omniphobic background. The obtained sizes of developed circle features are 7.4 ± 1.9 , 9.9 ± 1.4 , 11.9 ± 0.2 , and 13.9 ± 0.2 μm . Smallest developed areas are circles with 7.4 ± 1.9 μm size, smallest polymerized area is space between numbers which is 5 ± 0.7 μm in size. B) EDX mapping of Si of the same micropattern. $98.2 \pm 0.6\%$ silicon content was measured inside the omniphilic spots exposing the silicon substrate. C) EDX mapping of carbon (carbon K-alpha line signal marked in red). $1.6 \pm 0.4\%$ carbon content was measured inside the omniphilic spots. D) AFM analysis of a round spot border ($d = 40$ μm). i) AFM topography scan across the omniphilic (developed) and omniphobic (GPOSS-PDMS polymer coating) areas, demonstrating a sharp border. ii) Phase image of the spot border. Differences in phases correspond to different materials inside and outside of the spot. iii) Height profile corresponding to (D-i). Scale bars in A, B, and C are 80 μm , and in D 4 μm .

photolithography.^[30,31] This method allowed us to achieve sub-micron resolution to create an array of polymerized GPOSS-PDMS dots (Figure S7, Supporting Information). However, this method cannot be used to create wettability patterns with polymerized GPOSS-PDMS background.

2.4. Application of GPOSS-PDMS Micropatterns

One of many possible applications of wettability micropatterns is the use of hydrophilic areas surrounded by hydrophobic regions to confine liquids or to use the effect of discontinuous dewetting to create arrays of liquid droplets without the use of liquid dispensers. Here, the omniphobic nature of GPOSS-PDMS allows to confine not only aqueous droplets in hydrophilic spots but also droplets of low surface tension liquids. The effect of discontinuous dewetting could be achieved using hexadecane, DMF, and DMSO (Figure 5A,B). Figure 5B shows that DMSO forms the biggest droplets, followed by DMF and hexadecane, which correlates with their surface tensions: DMSO – 43.0 mN m^{-1} , DMF – 35.3 mN m^{-1} , and hexadecane – 27.5 mN m^{-1} . We have measured volume homogeneity of droplets produced by discontinuous dewetting for water (83 ± 5 nL), DMSO (40 ± 2 nL), and DMF (34 ± 4 nL). However, the volume of droplets generated by discontinuous dewetting depends also on the application speed, size of the source droplet, size

of hydrophilic patterns, distance between them, which makes it challenging to control. Direct application with a liquid dispenser is more controllable and reproducible. We obtained the following values of droplet volumes: 270 ± 20 , 179 ± 6 , and 127 ± 8 nL for water, DMSO, and DMF, respectively.

Herein, we demonstrate dispensing of 160 nL volumes of methylene blue aqueous solution into 1×1 mm square omniphilic spots using a non-contact liquid dispenser (Figure 5C(i)). We also dispensed an array of 5 μL methylene blue solution with a concentration range on a pattern with circles ($d = 3$ mm) (Figure 5C(ii)). The maximum volume of water that could be deposited into 1×1 mm omniphilic squares was 200 nL. The limiting volume of water that could be confined within the circles ($d = 3$ mm) was estimated to be 8 μL .

2.5. Cell Cultivation

Omniphobic coatings, slippery lubricant infused coatings, and even superhydrophobic coatings have been known to reduce cellular adhesion or to enhance cellular detachment, which was shown for both eukaryotic cells and prokaryotes.^[32–36] In this work, we investigated the cell adhesive or repellent properties of the GPOSS-PDMS and compared these properties to those of the omniphilic spots on our patterned surface. For this experiment, we used the mouse myoblast cell line C2C12.

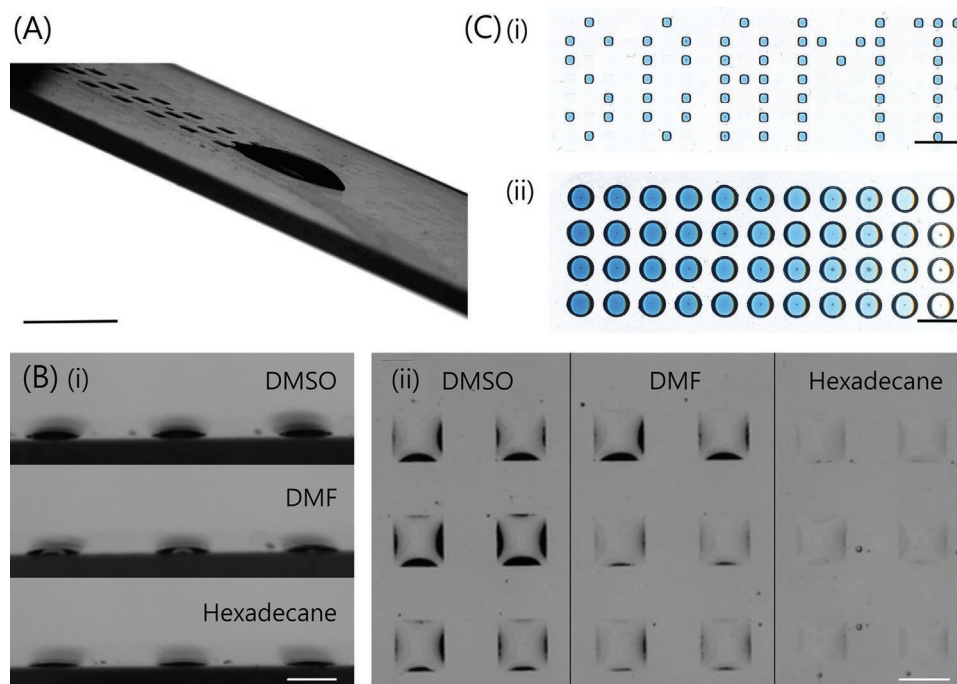


Figure 5. Application of various liquids as droplet microarrays for GPOSS-PDMS wettability patterns. A) Application of hexadecane to the wettability pattern via discontinuous dewetting. Scale bar is 5 mm. B) Solvents (DMSO, DMF, and hexadecane) were applied to the wettability pattern via discontinuous dewetting. i) Side view. Scale bar is 5 mm. ii) Top view. Scale bar is 5 mm. C) Examples of droplet arrangement on chips: i) Water solution of methylene blue applied to wettability patterns with the iDOT MINI liquid dispenser. Scale bar is 1 mm. ii) An aqueous solution of methylene blue was applied in a concentration gradient. Scale bar is 1 mm.

First, a pattern of 1 mm spots, separated by 1 mm GPOSS-PDMS (750 nm, composition A) was prepared on a glass substrate. The chip was immersed into a DMEM and seeded with C2C12 cells. After incubation for 24 h, the cells formed a monolayer on the surface of the entire chip (Figure S8A–D, Supporting Information). However, 96% of the cells located inside the omniphobic area detached upon gentle washing with PBS (Figure S8E–H, Supporting Information), while 99% of the cells remained in the omniphilic areas, resulting in a pattern of cells occupying the omniphilic spots. It should be noted that despite weak adhesion to the omniphobic surface, the cells had a normal morphology indicating absence of cytotoxicity of GPOSS-PDMS coating. In addition, almost no PI-positive cells were noted (99% viability) in the hydrophilic areas, confirming the biocompatibility of the coating. The cells fixed in the spots on the glass surface (Figure 6) did not differ in morphology from the cells on the omniphobic part. This method demonstrates a simple method for cell patterning using the omniphilic-omniphobic GPOSS-PDMS chip.

3. Conclusion

In this study, we demonstrate a new method for creating omniphobic-omniphilic micropatterns using GPOSS-PDMS coating. The surface omniphobicity of the coatings applied by photolithography was demonstrated by contact angle measurements. We have shown that the GPOSS-PDMS-based composition acts as a negative photoresist, making it possible to create an omniphobic-omniphilic pattern in one step. The simplified

photolithography protocol based on the use of a conventional UV source was shown to produce omniphobic patterns with 1 mm features. Solvents with a wide range of surface tensions, such as DMSO, DMF, and hexadecane, could be applied to the chip to form arrays of droplets by discontinuous dewetting. Both discontinuous dewetting and direct droplet dispensing could be demonstrated. The minimum size of the created structure was 8 μm . The GPOSS-PDMS composition could be used as a durable omniphobic photoresist. Omniphilic-omniphobic wettability patterns, which can be prepared without the use of specialized equipment, can be used for applications where confinement of liquids, miniaturization, and parallelization of chemical or biological experiments are important. We have shown that it can be used to grow adherent cell cultures, specifically in omniphilic spots. This approach can be used to form cell patterns, which might find applications to study cell migration or perform single cell studies. Further improvement of this method may further decrease the feature size and increase the difference in wettability between the omniphobic and omniphilic areas. In addition, increasing the mechanical and chemical resistance of the surface will make it possible to create reusable patterned substrates for the abovementioned applications.

4. Experimental Section

Chemicals: 3-Glycidyloxypropyl polyhedral oligomeric silsesquioxane (GPOSS) was purchased from Hybrid Plastics (Hattiesburg, MS, USA). Monoaminopropyl-terminated polydimethylsiloxane 18–25 cSt (PDMS-NH₂) was purchased from Gelest (Morrisville, PA, USA). A mixture of triarylsulfonium hexafluoroantimonate (50 wt.% in

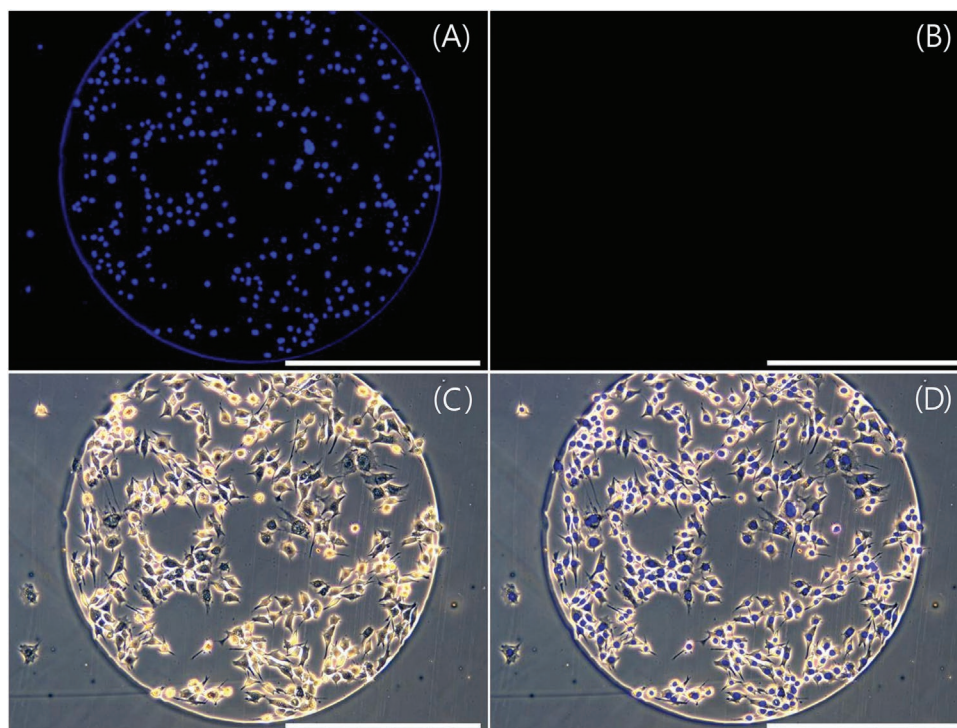


Figure 6. Images of C2C12 cells incubated on the omniphobic-omniphilic chip. A) Staining with Hoechst 33342; B) staining with propidium iodide (PI); C) phase-contrast image; D) merge of all images. As can be seen, no dead cells were observed inside omniphilic spots. Most cells (96%) attached to the omniphobic surface were washed away with a buffer solution. However, these cells were also viable (Figure S8C,G, Supporting Information). Scale bar is 500 μm .

propylene carbonate) and propylene carbonate was purchased from Sigma–Aldrich (St. Louis, MO, USA). Butyl acetate, ethanol, methanol, hexadecane, DMSO, DMF, acetone, and acetonitrile were used as received from Lenreactive (St. Petersburg, Russia). DMEM culture medium, FBS, PBS, and antibiotics were purchased from Biotol (St. Petersburg, Russia).

Preparation of GPOSS-PDMS Patterns: Substrates Preparation: 1) Glass slides activation: commercially available glass slides ($76 \times 26 \text{ mm}$) were placed in a 1 M solution of sodium hydroxide for 1 h. The slides were then transferred into hydrochloric acid (5 wt.%) for 20 min. The glass slides were then thoroughly rinsed with deionized water and dried with an air gun. The glass slides were used immediately after activation. 2) Silicon wafer preparation: silicon wafers (Telecom-STV, Zelenograd, Russia) were cut into squares ($2 \times 2 \text{ cm}$). The obtained pieces were subsequently ultrasonicated in acetone (10 min), isopropyl alcohol (10 min), and water (10 min). The clean wafers were used immediately after drying with an air gun.

Synthesis of GPOSS-PDMS Colloidal Solution: In a round bottom flask, GPOSS cage mixture (1.00 g; 0.75 mmol) was dissolved in butyl acetate (2 mL). PDMS-NH₂ (55 mg, 0.0275 mmol) was then added to the obtained solution (Figure 1A(i)). The mixture was heated under reflux at 110 °C for 1.5 h. The reaction mixture containing GPOSS-PDMS and unreacted GPOSS was cooled to room temperature and poured into acetonitrile (14 mL) (Figure 1A(ii)). The obtained solution was centrifuged at $1.60 \times 10^4 \text{ g}$ for 1 min. The supernatant was then separated by decantation.

Precursor Solution Preparation: For macropattern fabrication (Figure 3), precursor solution A was prepared as a mixture of 60 mg of GPOSS, 1 mL of GPOSS-PDMS colloidal solution prepared in the previous step, 200 μL of propylene carbonate, and 10 μL of photoinitiator solution (mixed salts of triarylsulfonium hexafluoroantimonate 50 wt.% in propylene carbonate).

For the micropatterning studies (see Figure 4), precursor solution B was prepared as a mixture of 60 mg of GPOSS cage mixture, 1 mL of GPOSS-PDMS colloidal solution, 200 μL of propylene carbonate, and 43 μL of photoinitiator solution.

Photolithography Process: Coating Application: To fabricate macropatterns, precursor solution A (500 μL) was evenly spread over an activated glass slide ($76 \times 26 \text{ mm}$ size) and then spin-coated with POLOS SPIN150i at 1000 rpm for 1 min. For the micropatterning studies, precursor solution B (120 μL) was drop-casted and spin-coated on clean silicon wafers (square samples of $10 \times 10 \text{ mm}$ size) at 1000 rpm for 1 min.

Photolithography of Macro Patterns: At the end of the spin-coating process, a glass slide was placed on a heating plate and dried at 80 °C for 10 min. Then, the dried coating was irradiated with a high-pressure mercury vapor lamp (125 W, wavelength range from 254 to 579 nm, 6.9 mW cm^{-2} at a wavelength of 365 nm, 10 cm distance between the source and the substrate) for 8 min using a lime glass-chromium photomask (the thickness of the metal mask was $\approx 100 \text{ nm}$). The pattern was developed in acetone for 30 s. The developed patterns were additionally irradiated with the same high-pressure mercury vapor lamp for 15 min without any slide covering to ensure complete polymerization.

Photolithography of Micropatterns: Silicon wafers with spin-coated GPOSS-PDMS layers were dried on a heating plate at 90 °C for 10 min. The substrates were then exposed to UV light for 25 min using a SÜSS MicroTec MJB4 mask-aligner (Garching, Germany) (a wavelength of 365 nm and a power of 0.9 mW cm^{-2}). The exposed coatings were post baked on a heating plate at 90 °C for 5 min. Subsequently, the patterns were developed in acetone for 30 s and dried.

Microsphere Photolithography: A monolayer of 3 μm in diameter polystyrene spheres was spin-coated on a thin film of GPOSS covering a Si substrate. The substrates were then exposed to UV light with 365 nm wavelength and $1.5 \mu\text{J cm}^{-2}$ exposure dose. The patterns were developed in acetone for 30 s.

Cell Experiments: The mouse myoblast cell line C2C12 (Institute of Cytology Russian Academy of Science, St. Petersburg, Russia) was used to evaluate cell adherence to patterns. The GPOSS-PDMS macropatterned slides were sterilized with 70% ethanol for an hour and then placed in sterile Petri dishes. Then, 5 mL of the culture medium (DMEM + 10% FBS + Pen/Strep) was added to the Petri dish. Further, 2 mL of suspension of C2C12 cells was added and the dish was placed in an incubator (37 °C, 5% CO₂) for 24 h. After incubation, the cells were stained with a mixture of Hoechst 33 342 and propidium iodide by direct addition of the dyes to the medium (final concentrations of 10 µg mL⁻¹ each). After 20 min, the slides were washed with phosphate-buffered saline (PBS). The cells were visualized under a Leica DMi 8 microscope (Leica Microsystems CMS, Wetzlar, Germany).

Characterization Methods: The surface of the macropatterned slides was characterized by contact angle measurements using a Drop Shape Analyzer DSA25 (Krüss GmbH, Hamburg, Germany). The apparent static contact angles were measured using the Young Laplace fitting method by applying 4 µL droplets of various liquids (ethanol, hexadecane, DMF, DMSO, and water) on omniphilic or omniphobic areas. Advancing contact angles were measured with the following method.^[3] Briefly, a 2 µL droplet of the tested liquid was applied to the surface of a sample. The source needle was placed halfway inside the droplet from the perspective of the camera in the middle of the droplet. Subsequently, 1 µL of the liquid was dispensed at a flow rate of 0.05 µL s⁻¹. In the last stage, the dispensation of an 8 µL volume at a flow rate of 0.05 µL s⁻¹ was recorded. The recorded images were analyzed. The final advancing contact angle was calculated as the average of the contact angle values obtained from each image in the measurement. Receding contact angles were measured according to the following method.^[3] Briefly, the dispenser needle was placed close to the sample surface without touching it. A 13 µL droplet was applied to the surface of the sample at a flow rate of 2 µL s⁻¹. Subsequently, 2 µL of the liquid was removed from the droplet at a flow rate of 0.05 µL s⁻¹. At the last stage of the measurement, the liquid was taken at a flow rate of 0.05 µL s⁻¹ until complete removal. Images recorded during the last stage of the measurement were analyzed. The final receding contact angle was calculated as the average of the contact angle values obtained from each image in the measurement. The sliding contact angles were measured using the following procedure: volumes (5, 10, 15, and 20 µL) of different liquids (ethanol, hexadecane, DMSO, and DMF) were placed on the omniphobic surface, and the tilt angle was gradually changed (0.3° s⁻¹) until the droplet movement was registered using a DSA25 camera. The maximum volume of solvent that can be applied to 1 mm circular omniphilic spots was measured using the following method. The tested solvent was added at a rate of 50 nL s⁻¹ using DSA25. Droplet volume was measured when the droplet crossed the border of the omniphilic spot. The average droplet volume applied by the discontinuous dewetting method was determined as follows. A drop of solvent was applied to the wettability pattern placed at a fixed angle. The mass of the drop was measured before and after application. The difference in drop mass was divided by the number of droplets applied.

Optical scanning of the chips was performed using an Epson Perfection V600 Photo scanner. Scanning electron microscopy (SEM) and energy dispersive X-ray (EDX) analyses were performed using a VEGA 3 SBH (Brno, Czech Republic). Atomic force microscopy (AFM) analyses were performed using an NT-MDT Solver NEXT (NT-MDT, Russia) in the non-contact mode. The images were obtained using cantilever with force constant of 34 N m⁻¹ and resonance frequency of 345 kHz. Optical microscopy of patterns was performed on Leica DMi8 (Leica Microsystems CMS, Wetzlar, Germany) in phase contrast mode with 100 W constant color temperature LED illumination.

Supporting Information

Supporting Information is available from the Wiley Online Library or from the author.

Acknowledgements

The work of D.K. and I.L. was supported by RSF grant no. 22-73-00111. The work of A.P., A.K., and E.S. was supported by the national project "Science and Universities", project No. FSER-2022-0008. A.G. thanks the RSF grant no. 21-79-10202 for the support of the study of resist patterning. P.A.L. thanks the DFG (Heisenbergprofessur Projektnummer: 406232485, LE 2936/9-1) for the financial support.

Open access funding enabled and organized by Projekt DEAL.

Conflict of Interest

The authors declare no conflict of interest.

Data Availability Statement

The data that support the findings of this study are available from the corresponding author upon reasonable request.

Keywords

colloid chemistry, droplet manipulation, droplet microarray, NP-GLIDE, omniphobic surfaces, photolithography, polymer chemistry, wettability patterns

Received: February 19, 2023

Revised: March 22, 2023

Published online: April 18, 2023

- [1] Z. Chu, S. Seeger, *Chem. Soc. Rev.* **2014**, *43*, 2784.
- [2] M. A. Samaha, M. Gad-el-Hak, *Phys. Fluids* **2021**, *33*, 071301.
- [3] T. Huhtamäki, X. Tian, J. T. Korhonen, R. H. A. Ras, *Nat. Protoc.* **2018**, *13*, 1521.
- [4] W. Niu, G. Y. Chen, H. Xu, X. Liu, J. Sun, *Adv. Mater.* **2022**, *34*, 2108232.
- [5] J. Yin, M. L. Mei, Q. Li, R. Xia, Z. Zhang, C. H. Chu, *Sci. Rep.* **2016**, *6*, 25924.
- [6] H. J. Cox, C. P. Gibson, G. J. Sharples, J. P. S. Badyal, *Adv. Eng. Mater.* **2022**, *24*, 2101288.
- [7] P. Zhu, T. Kong, X. Tang, L. Wang, *Nat. Commun.* **2017**, *8*, 15823.
- [8] T.-S. Wong, S. H. Kang, S. K. Y. Tang, E. J. Smythe, B. D. Hatton, A. Grinthal, J. Aizenberg, *Nature* **2011**, *477*, 443.
- [9] L. Wang, T. J. McCarthy, *Angew. Chem., Int. Ed.* **2016**, *55*, 244.
- [10] K. Zhang, S. Huang, J. Wang, G. Liu, *Angew. Chem., Int. Ed.* **2019**, *58*, 12004.
- [11] W. Feng, E. Ueda, P. A. Levkin, *Adv. Mater.* **2018**, *30*, 1706111.
- [12] A. A. Popova, T. Tronser, K. Demir, P. Haitz, K. Kuodyte, V. Starkuviene, P. Wajda, P. A. Levkin, *Small* **2019**, *15*, 1901299.
- [13] M. Tsotsalas, H. Maheshwari, S. Schmitt, S. Heißler, W. Feng, P. A. Levkin, *Adv. Mater. Interfaces* **2016**, *3*, 1500392.
- [14] M. Benz, A. Asperger, M. Hamester, A. Welle, S. Heissler, P. A. Levkin, *Nat. Commun.* **2020**, *11*, 5391.
- [15] I. You, T. G. Lee, Y. S. Nam, H. Lee, *ACS Nano* **2014**, *8*, 9016.
- [16] J. Bruchmann, I. Pini, T. S. Gill, T. Schwartz, P. A. Levkin, *Adv. Healthcare Mater.* **2017**, *6*, 1601082.
- [17] S. P. R. Kobaku, A. K. Kota, D. H. Lee, J. M. Mabry, A. Tuteja, *Angew. Chem.* **2012**, *124*, 10256.
- [18] Y.-K. Lai, Y.-X. Tang, J.-Y. Huang, F. Pan, Z. Chen, K.-Q. Zhang, H. Fuchs, L.-F. Chi, *Sci. Rep.* **2013**, *3*, 3009.
- [19] W. Feng, L. Li, X. Du, A. Welle, P. A. Levkin, *Adv. Mater.* **2016**, *28*, 3202.

- [20] C. Zheng, G. Liu, H. Hu, *ACS Appl. Mater. Interfaces* **2017**, *9*, 25623.
- [21] M. Rabnawaz, G. Liu, H. Hu, *Angew. Chem., Int. Ed.* **2015**, *54*, 12722.
- [22] M. Rabnawaz, G. Liu, *Angew. Chem., Int. Ed.* **2015**, *54*, 6516.
- [23] S. Arscott, *Lab. Chip.* **2014**, *14*, 3668.
- [24] B. Bohl, R. Steger, R. Zengerle, P. Koltay, *J. Micromech. Microeng.* **2005**, *15*, 1125.
- [25] R. J. Jackman, D. C. Duffy, E. Ostuni, N. D. Willmore, G. M. Whitesides, *Anal. Chem.* **1998**, *70*, 2280.
- [26] K. Zhang, S. Huang, J. Wang, G. Liu, *Angew. Chem., Int. Ed.* **2019**, *58*, 12004.
- [27] G. Vazquez, E. Alvarez, J. M. Navaza, *J. Chem. Eng. Data* **1995**, *40*, 611.
- [28] L. D. Eske, D. W. Galipeau, *Colloids Surf. A Physicochem. Eng. Asp* **1999**, *154*, 33.
- [29] E. Gee, G. Liu, H. Hu, J. Wang, *Langmuir* **2018**, *34*, 10102.
- [30] L. N. Dvoretckaia, A. M. Mozharov, Y. Berdnikov, I. S. Mukhin, *J. Phys. D Appl. Phys.* **2021**, *55*, 09LT01.
- [31] L. Dvoretckaia, V. Gridchin, A. Mozharov, A. Maksimova, A. Dragunova, I. Melnichenko, D. Mitin, A. Vinogradov, I. Mukhin, G. Cirlin, *Nanomaterials* **2022**, *12*, 1993.
- [32] D. C. Leslie, A. Waterhouse, J. B. Berthet, T. M. Valentin, A. L. Watters, A. Jain, P. Kim, B. D. Hatton, A. Nedder, K. Donovan, E. H. Super, C. Howell, C. P. Johnson, T. L. Vu, D. E. Bolgen, S. Rifai, A. R. Hansen, M. Aizenberg, M. Super, J. Aizenberg, D. E. Ingber, *Nat. Biotechnol.* **2014**, *32*, 1134.
- [33] S. M. Imani, M. Badv, A. Shakeri, H. Yousefi, D. Yip, C. Fine, T. F. Didar, *Lab. Chip.* **2019**, *19*, 3228.
- [34] E. Ueda, P. A. Levkin, *Adv. Healthcare Mater.* **2013**, *2*, 1425.
- [35] F. L. Geyer, E. Ueda, U. Liebel, N. Grau, P. A. Levkin, *Angew. Chem., Int. Ed.* **2011**, *50*, 8424.
- [36] L. Xiao, J. Li, S. Mieszkien, A. Di Fino, A. S. Clare, M. E. Callow, J. A. Callow, M. Grunze, A. Rosenhahn, P. A. Levkin, *ACS Appl. Mater. Interfaces* **2013**, *5*, 10074.